

Glabridin from licorice alleviates vascular inflammation and promotes vascular remodeling of the left anterior descending coronary artery in diabetic rat heart

Udomlak Matsathit¹, Wipapan Khimmakong²

¹Department of Food Science and Nutrition, Faculty of Science and Technology, Prince of Songkla University, Pattani, Thailand

²Division of Health and Applied Sciences, Faculty of Science, Prince of Songkla University, Songkhla, Thailand

Submitted: 26 January 2021; **Accepted:** 26 April 2021

Online publication: 9 May 2021

Arch Med Sci

DOI: <https://doi.org/10.5114/aoms/136112>

Copyright © 2021 Termedia & Banach

Corresponding author:

Wipapan Khimmakong PhD

Division of Health
and Applied Sciences
Faculty of Science

Prince of Songkla University
Songkhla, Thailand

E-mail: wipapan.k@psu.ac.th

Abstract

Introduction: The aim of this study was to investigate the effects of glabridin on vascular inflammation and vascular remodeling of the left anterior descending artery (LAD) in diabetic rat heart.

Material and methods: Eighty male Wistar rats were divided into five groups: (1) control rats; (2) glabridin control rats that received diet supplemented with glabridin (CGB); (3) diabetic rats (STZ); (4) diabetic rats that received a supplemented with glabridin (STZ + GB) 40 mg/kg BW; and (5) diabetic rats treated with glyburide (STZ + GR) 4 mg/kg BW. Diabetic animals were rendered diabetic by injection of a single dose (60 mg/kg BW) of streptozotocin (STZ). After 8 weeks, the biochemical markers of oxidative stress were assessed. The three-dimensional morphology of LAD was examined by vascular corrosion casting. Enzyme-linked immunosorbent assay was applied to determine the expression of TNF- α and IL-1 β proteins. Western blot and immunofluorescence analysis were used to detect the expression of VEGF and TGF- β 1 secretions.

Results: The lumen diameter of the LAD was notably smaller and stenotic. LAD analysis revealed arterial notch and evolved irregular caliber. Moreover, neovascularization appeared and was extensive. The Trolox equivalent antioxidant capacities and Trolox equivalent antioxidant capacity levels of heart tissue were significantly decreased and levels of malondialdehyde were found to be elevated in STZ rats whereas they were improved in the STZ + GB group. Increased expression levels of VEGF, TGF- β 1, TNF- α , and IL-1 β proteins in heart tissues were observed in the STZ group. The inflammation cytokine levels were decreased in the STZ + GB group.

Conclusions: These results revealed that glabridin was able to reduce LAD and heart tissue damage. Glabridin can be an antioxidant and can reduce the pathology of the LAD in terms of reducing inflammation and restoring condition of the LAD. It would be beneficial in examining the role of glabridin as a therapeutic aim in diabetes treatment research in coronary artery disease.

Key words: diabetes mellitus, streptozotocin, glabridin, heart, left anterior descending artery.

Introduction

Diabetes mellitus (DM) has reached epidemic proportions worldwide with rising prevalence. DM is one of the metabolic dysfunctions caused

by insufficient insulin action or ineffective insulin production. Diabetic patients have a twofold higher risk of myocardial infarction (MI) and stroke than the general population [1, 2]. Coronary artery disease (CAD) is a major determinant of the long-term prognosis among diabetic patients. DM is associated with a two to four times increased mortality risk from heart disease. Furthermore, in patients with DM there is increased mortality after MI, and worse overall prognosis with CAD [3]. Diabetic patients have a high plaque burden mainly distributed in the coronary artery. The most common diseased coronary vessel is the left anterior descending (LAD) artery (anterior interventricular branch of the left coronary artery) and proximal segment of each coronary vessel [4]. LAD is mostly a blockage site with coronary arteries. Blockage of this artery is often called the widow-maker infarction due to a high mortality rate. This proximal critical blockage usually stops all the blood flow to the left side of the heart, normally causing the heart to stop beating and leading to cardiac arrest [5].

Myocardial ischemia represents a condition of suffering for cardiomyocytes due to reduced coronary blood flow as compared to their metabolic demand, and it may manifest through several clinical conditions. A blocked LAD may arise from coronary artery disease and hinder the impulse conduction between the atria and the ventricles. Myocardial infarction generally occurs when there is a critical blockage in one or more of the arteries that supply the heart muscle with blood. Within minutes at the completely occluded stage, the heart muscle stops working. If blood flow is not restored within minutes to hours, the muscle typically dies, leading to impairment or death of the conducting system [6].

The heart is a muscular organ that pumps blood through the body at an average of 72 times per minute. Oxygen and nutrients are carried to the heart in the form of blood that flows through the coronary arteries. The LAD coronary artery is almost always the largest of the branches of coronary arteries [7]. The LAD appears to be directly continued from the left coronary artery, which descends into the anterior interventricular groove. This artery carries almost 50% of the blood carried by the coronary circulation of the left ventricular myocardial mass, or approximately twice as much as either the right or the left circumflex coronary artery [8]. Branches of this artery, anterior septal perforating arteries, enter the septal myocardium to supply the anterior two-thirds of the interventricular septum. The great cardiac vein (GCV), the venous complement of the left anterior descending artery, runs in the anterior interventricular groove and drains the anterior aspect of the heart. It is the main tributary of the coronary sinus.

Vascular inflammation in the blood vessels can cause their walls to thicken, which reduces the width of the passageway through the vessel. Restricted blood flow may damage the organ and tissue. Vascular wall inflammation plays a key role in the pathogenesis of vascular disease and the atherosclerotic process [9]. The malfunctions of these vascular complications are related to the hyperglycemic metabolic alteration, endothelial dysfunction and increased oxidative stress and inflammation. The inflammatory reaction involves complex interactions between inflammatory cells, such as neutrophils, lymphocytes, monocytes/macrophages, and vascular cells. This interaction results in an inflammatory response by vascular cells through the increased expression of adhesion molecules, cytokines, chemokines, matrix metalloproteinases, and growth factors [9]. Proteins in the plasma and cell membrane are altered by chronic exposure to hyperglycemia through the process of nonenzymatic glycosylation, leading to the attachment of glucose molecules. Hyperglycemia-induced oxidative stress promotes the formation of advanced glycosylation end products (AGEs) and PKC activation [10]. Cardiovascular diseases are characterized by imbalanced formation of reactive oxygen species (ROS) and ROS-degrading antioxidant systems. This imbalance leads to the accumulation of superoxide, hydrogen peroxide, and other products such as peroxynitrite and hypochlorous acid and a deviation from the steady state [11].

Glabridin, the main active ingredient of licorice or *Glycyrrhiza glabra*, is a polyphenolic flavonoid that has an effect on the reduction of blood glucose levels [12]. It displays anti-proliferative, antimicrobial and anti-fatigue activities [13]. Glabridin exhibits superoxide-scavenging activity in biological membranes and is a potent antioxidative that can improve oxidative stresses in the mitochondrial electron transport system [14]. Glabridin also has the potential to recover the damaged hepatocytes and collagen accumulation in the extracellular matrix of the diabetic rat liver [15]. In this experimental study, we aimed to investigate the alleviating effects of glabridin on vascular inflammation and vascular remodeling of the LAD on histological, ultrastructural changes and to determine the levels of vascular endothelial growth factor (VEGF), transforming growth factor- β 1 (TGF- β 1), tumor necrotic factor- α (TNF- α) and interleukin- 1β (IL- 1β) protein expression and biochemical markers of oxidative stress in streptozotocin (STZ)-induced diabetic rats.

Material and methods

Animal treatment

The ethical approval of experimental procedures was licenced by the Animal Ethics Commit-

tee of the Prince of Songkla University, and the protocols were reviewed and approved (project number Ref.11/2018). The study was carried on 8-week-old male Wistar rats weighing approximately 200–250 g at the beginning of the experiment. They were purchased from Nomura Siam International Co., Ltd. All experiments were carried out in a controlled animal laboratory environment with alternating 12-hour light/dark periods (23 ±2°C) with lights on at 7:00 a.m. and humidity 50 ±10%.

Induction of type I diabetes

Diabetes in rats was induced by intraperitoneal injection of streptozotocin (STZ) (Sigma, St. Louis, MO, USA) (60 mg/kg BW) dissolved in 0.1 M citrate buffer, pH 4.5, while control rats received an injection with 0.1 M citrate buffer alone. Rats with blood sugar levels greater than 250 mg/dl were used as diabetic animals. Blood from the lateral tail vein was analyzed for blood sugar level using a blood glucose meter (Accu-Chek Active meter and test strips, Roche Diagnostics, Mannheim, Germany). Three days after the STZ injection, control and diabetic rats were randomly divided into five groups as follows: (1) normal control rats received a balanced standard diet (C); (2) glabridin control rats received a balanced standard diet supplemented with glabridin (purified > 98% by HPLC analysis) (Shaanxi Langrun Biotechnology Co., LTD., Xi'an, China) in 0.5 ml of 0.5% Tween 80 solution (CGB); (3) diabetic rats received a balanced standard diet (STZ); (4) diabetic rats received a balanced standard diet supplemented with glabridin (STZ + GB) 40 mg/kg BW in 0.5 ml of 0.5% Tween 80 solution, and (5) diabetic rats were treated with glyburide (STZ + GR) 4 mg/kg BW in 0.5 ml of 0.5% Tween 80 solution to demonstrate the effectiveness of glabridin. All animals were weighed and clinically observed on a weekly basis. After glabridin supplementation at the end of 8 weeks, experimental rats ($n = 80$ in all groups) were euthanized with an overdose of thiopental sodium (150 mg/kg) (intraperitoneal injection). The blood was collected from the heart for biochemical assay and analyzed for blood cholesterol by the Southern Lab Center Saha Clinic (Songkhla, Thailand; using a Siemens ADVIA 1800 System Analyzer; Siemens Healthiness, Erlangen, Germany). The heart tissues were removed and collected for histological, ELISA and immunofluorescence studies ($n = 40$), and injected with resin for vascular casting combined with SEM ($n = 40$).

Total antioxidant capacity determination

The total antioxidant capacity of heart tissue hydrolysate was assayed using 2,2'-azino-bis(3-eth-

ylbenzothiazoline-6-sulfonic acid (ABTS) according to the previously reported protocol [16] with some modifications. 30 mg of heart tissue were homogenized in 500 μ l of 1xRIPA buffer and centrifuged at 10000xg for 15 min at 4°C and then the supernatant was collected for assay. 7 mM ABTS radical mixture was produced using 2.45 mM potassium persulfate (final concentration) and the mixture was allowed to stand in the dark at 4°C for 12–16 h before use. The amount of ABTS⁺ produced can be monitored by reading absorbance at 734 nm and it was diluted with 1x phosphate buffer saline pH 7.4 (PBS) until it reached 0.7±0.02. For the reaction, 20 μ l of sample and standard solution were added to a 96-well plate and subsequently mixed with 180 μ l of ABTS radical solution. The reaction mixture was incubated at room temperature in the dark for 3 min. The absorbance was measured at 734 nm. Total antioxidant capacity was calculated according to the following equation: % inhibition = $(1 - \text{OD sample}/\text{OD blank}) \times 100$.

The antioxidant capacity of heart tissue homogenate was calculated as percentage inhibition of ABTS⁺. A Trolox standard curve was used as a reference and the results were expressed as Trolox equivalent antioxidant capacity (TEAC) per milligram of tissue samples.

Determination of malondialdehyde (MDA) levels

The MDA levels were measured using the Lipid Peroxidation (MDA) Assay Kit (Sigma-Aldrich, St. Louis, MO, USA, Cat. No. MAK085) in accordance with the manufacturer's protocols. Briefly, heart tissue (30 mg) was homogenized with homogenizer on ice in 900 μ l of MDA lysis buffer containing 9 μ l of 100xBHT, then centrifuged at 13,000xg for 10 min to remove insoluble material. An aliquot of heart tissue homogenates (200 μ l) was placed into a microcentrifuge tube, followed by adding 600 μ l of the TBA solution into each vial containing the standard and sample to form the MDA-TBA adduct. It then was heated at 95°C for 60 min and then cooled to room temperature in an ice bath for 10 min. After cooling, the reaction mixture (200 μ l) was transferred into 96-well plates, and the absorbance was determined using a spectrophotometer at 532 nm against distilled water. The results were reported as nmol/mg tissue.

Histological preparation

The hearts were fixed in 10% formaldehyde overnight and then dehydrated in a graded series of ethanol through 70, 80, 90, 95, and 100% with two changes for 1 h each. Three changes of xylene with 30 minutes each were used as a clearing reagent before filtration. The tissue was em-

bedded in paraffin, sectioned at 5 μm thick, and then stained with hematoxylin and eosin (H&E). All sections were examined and photographed using an Olympus light microscope (BX-50, Olympus, Japan).

Determination of inflammatory cytokine by ELISA

The heart tissues of rat were homogenized with homogenizer on ice for at least 90 s in 500 μl of RIPA buffer (Sigma-Aldrich, St. Louis, MO, USA) plus 1% of protease inhibitor cocktail (Sigma-Aldrich, St. Louis, MO, USA). After clarification by centrifugation for 15 min at 12,000 \times g, 4°C, TNF- α and IL-1 β levels were assessed using the ELISA kits (Sigma-Aldrich, St. Louis, MO, USA, Cat. No. RAB0480 and No. RAB0278, respectively). This assay employs an antibody specific for rat TNF- α and IL-1 β by following the manufacturer's protocols. Briefly, 100 μl of samples were pipetted into an ELISA-well plate pre-coated with rat TNF- α and IL-1 β antibodies and incubated for 2.5 h at room temperature with gentle shaking. After that, the wells were washed with wash buffer and biotinylated anti-rat TNF- α and IL-1 β antibodies were added to each well. After washing away the unbound biotinylated antibody, 100 μl of the HRP-conjugated streptavidin were pipetted to the wells and incubated for 45 min at room temperature. All wells were again washed, 100 μl of a TMB substrate solution was added, and it was incubated for 30 min. Finally, the stop solution was added, and the color changed from blue to yellow. Finally, the optical density of each well was determined within 30 min, using a spectrophotometer (Multiskan, Finland) at 450 nm. Each sample was tested in duplicate.

Immunofluorescence study

For fluorescent microscopy imaging of VEGF and TGF- β 1, heart tissues were fixed with 10% formaldehyde. Paraffin sections were cut as 5 μm sections, deparaffinized in xylene, hydrated through graded ethanol to distilled water, and permeabilized in PBS with 0.1 Triton X-100 (PBST) for 30 min. Blocking was performed using horse serum in PBS for 1 h at room temperature, followed by incubation with mouse monoclonal anti-VEGF antibody (VG1) (Thermo Fisher Scientific, Waltham, MA, USA) mixed with rabbit anti-TGF- β 1 (Abcam, Cambridge, UK) and diluted 1 : 100 in blocking serum at 4°C overnight. After washing three times with PBS, the sections were exposed to the Fluorescein Horse Anti-Mouse IgG Antibody (1 : 200; Vector Laboratories, USA) and used to detect VEGF and Texas Red Goat Anti-Rabbit IgG (H + L) Antibody (1 : 200; Vector Laboratories, USA) in

blocking solution to detect TGF- β for 2 h at room temperature in the dark. The images were examined under a fluorescence microscope (BX-50, Olympus, Japan). The VEGF and TGF- β percentage of cell expression was determined by the National Institutes of Health (NIH) Image J software 1.52 to measure fluorescent intensity. Five LADs were randomly selected in each specimen. Optical density (OD) of each was normalized by LAD area ImageJ 1.52 software and used to measure the level of immunostaining at the area of LADs. The X400 images were converted to 8-bit grayscale and selected. Area and integrated density, and background intensity were measured by selecting three distinct areas in the background with no staining. The optical density (OD) was determined as: $OD = ID - (A \times MGV)$, where ID is the integrated density of the selected glomerular region, A is the area of the selected glomerular region, and MGV is the mean gray value of the background readings), and then the mean OD of these glomeruli was taken for statistical analysis [17].

Vascular corrosion cast examination

Rats were injected with an overdose of thiopental sodium (150 mg/kg) (IP injection) at the end of the experiment. 0.5 ml (5,000 IU/ml) of heparin was quickly injected into the left ventricle and its tip directed towards the lumen of the ascending aorta with a blunt no. 18 gauge needle. Approximately 300 ml of 0.9% NaCl solution was infused through a cannula until the effluent was clear. PU4ii resin (VasQtec, Zürich, Switzerland) was immediately injected into the cannula through the ascending aorta. The heart was removed from each animal and immersed in warm water (80°C) to assure polymerization of the plastic. They were immersed in 10% KOH for 30 days to let the tissue break up, leaving a casting of the vessels. The specimens were washed several times with distilled water. The vascular cast could dry in the air. Finally, the casts were examined under the scanning electron microscope (JEOL JSM-5400) at accelerating voltage of 10 kV. The diameter of heart blood vessels was measured by SemAfore, 5.2.

Western blotting analysis

Western blotting analysis of VEGF and TGF- β 1. The heart tissues of rats in 8-week lysates of control, CGB, STZ, STZ + GB and STZ + GR groups were prepared in ice-cold RIPA buffer (Sigma-Aldrich; Merck KGaA) supplemented with 1 \times protease inhibitor cocktails (Merck Millipore, Bedford, MA, USA). To collect the supernatants, the homogenates were centrifuged at 14,000 \times g for 30 min at 4°C. The protein concentration of the supernatant was estimated by BCA protein assay kit (Pierce

biotechnology, Rockford, IL, USA). Total protein (10 µg) was diluted (1 : 2) in treatment buffer (0.125 M Tris-Cl, 4% SDS, 20% glycerol, 10% 2-mercaptoethanol and 0.2% bromophenol blue) and heated for 5 min. Protein samples were subjected to 12% polyacrylamide gel electrophoresis (100 V, 0.35 A and 300 W for 90 min) and subsequently transferred onto nitrocellulose membranes (GE Healthcare, Chicago, IL, USA). Membranes were blocked with 5% non-fat dry milk in 0.1% Tris buffered saline with Tween (TBS-T) for 1 h. The membranes were incubated with primary antibodies against VEGFA (1 : 500; Rabbit monoclonal (EP1176Y) to VEGFA ab 52917), (Abcam, Cambridge, MA, USA), anti-TGF-β1 antibody (1 : 1000; Rabbit polyclonal Antibody) (ab92486, Abcam, Cambridge, MA, USA) and β-actin (1 : 3000; Rabbit polyclonal ab8227) (Abcam, Cambridge, MA, USA) at 4°C for 24 h. Membranes were washed three times with TBS-T, followed by incubation for 2 h at room temperature with a goat anti-rabbit horse-radish peroxidase-conjugated immunoglobulin G (1 : 5000; ab6721; Abcam Cambridge, MA, USA) which was used as a source of secondary antibodies. Finally, protein bands were visualized using the enhanced chemiluminescence (ECL) detection system and ECL film (GE Healthcare, Chicago, IL, USA) GE Healthcare), while the immune complexes were detected using ImageJ software (version 1.50, NIH, <https://imagej.nih.gov/ij/>, Bethesda, MD, USA) which was used to quantify the integrated density.

Statistical analysis

The results were expressed as mean ± standard error of the mean. Statistical analysis was

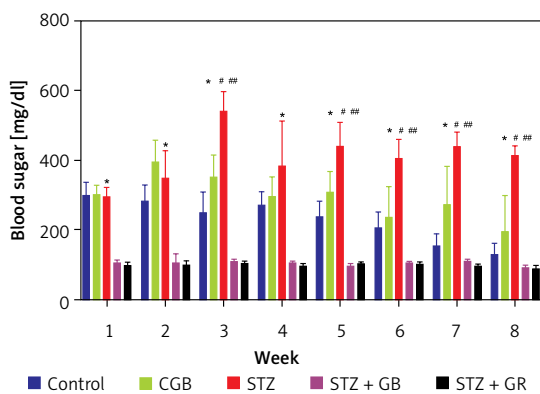


Figure 1. Blood sugar levels of control, CGB, STZ, STZ + GB and STZ + GR groups for a period of 8 weeks. The blood sugar levels significantly elevated in the STZ, STZ + GB and STZ + GR groups compared with the control and CGB rats ($p < 0.001$). Furthermore, blood sugar levels of STZ + GB rats and STZ + GR rats significantly decreased every week compared with STZ rats ($p < 0.01$ and $p < 0.001$, respectively). Values are mean ± SE, * $p < 0.001$

performed using ANOVA followed by Bonferroni posttest. A p -value smaller than 0.05 was considered as statistically significant. Graph Pad Prism 8.0 (GraphPad Software, USA) was used to perform statistical analysis.

Results

Effect of glabridin on blood sugar and cholesterol levels

The effect of glabridin on blood sugar levels of all rats was studied for 8 weeks. The blood sugar levels in the control, CGB, STZ, STZ + GB and STZ + GR groups are demonstrated in Figure 1. The results indicate that blood sugar levels were significantly elevated in the STZ, STZ + GB and STZ + GR groups compared with the control and CGB rats ($p < 0.001$). Furthermore, blood sugar levels of STZ + GB rats and STZ + GR rats significantly decreased weekly compared with STZ rats ($p < 0.01$ and $p < 0.001$, respectively).

Figure 2 presents the effect of glabridin on cholesterol levels in diabetic rats at 8 weeks. The cholesterol levels were significantly increased in the STZ group ($p < 0.05$) compared with the control rats. After supplementation of glabridin, cholesterol levels reduced in STZ + GB and GR groups compared with the STZ rats.

Histological observations of LAD

Histological analysis and wall thickness of LAD in the control, CGB, STZ, STZ + GB and STZ + GR groups are presented in Figures 3 A and 3 B. The wall of the LAD demonstrated increased collagen thickness (Figures 3 Ac, h) and stained blue collagen fibers in tunica media and tunica adventitia (Figure 3 Ah) in the STZ group. Moreover, the lumen diameter of LAD had a notably smaller LAD lumen and presented stenosis. Decreased collagen fiber accumulation in STZ + GB and STZ + GR rats was found. The wall thickness of the LAD in STZ rats

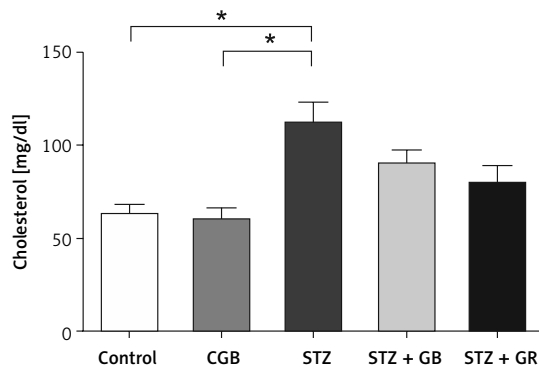


Figure 2. Average cholesterol levels of control, CGB, STZ, STZ + GB and STZ + GR groups at 8 weeks. Cholesterol levels were significantly elevated in the STZ group versus the control group. Values are mean ± SE, * $p < 0.001$

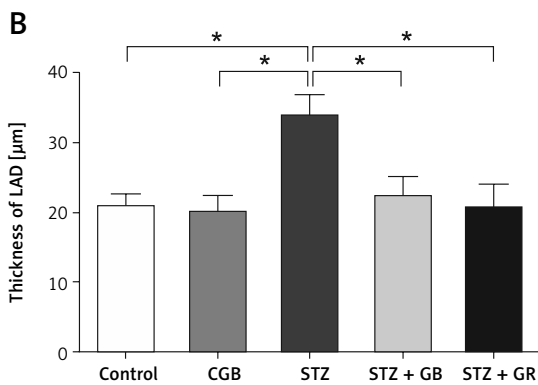
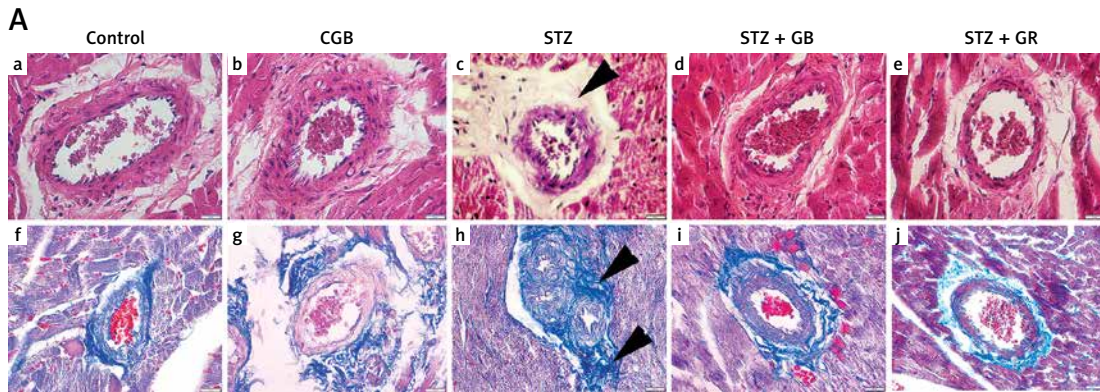


Figure 3. A – Light micrographs of LAD in heart tissue of rats were stained with H&E (a–e) and Masson’s trichrome techniques (f–j). Black arrowheads indicate the accumulation of collagen fibers. **B** – Average thickness of LAD in five group of rats at 8 weeks is shown. Values are mean ± SE, ****p* < 0.001 compared with control group and STZ group

was significantly increased (*p* < 0.001) compared with control and CGB groups. In contrast, it was significantly decreased in supplemented STZ + GB rats and STZ + GR rats (*p* < 0.001).

Total antioxidant capacity determination

The antioxidant capacities of cardiac tissue homogenate of the different groups are shown in Figure 4 A. The TEAC levels in diabetic in STZ rats were significantly decreased compared with control and CGB groups (*p* < 0.05 and *p* < 0.001 respectively). Also, treated diabetic rats in STZ + GB and STZ + GR groups had slightly higher TEAC

levels (*p* < 0.05 and *p* < 0.001 respectively) compared to diabetic rats. The TEAC levels of glabridin-treated rats remained unchanged compared to normal rats.

Determination of malondialdehyde (MDA) levels

Diabetic rats exhibited an increase in cardiac MDA levels compared to control and CGB rats (*p* < 0.01). Following treatment with glabridin and glyburide in STZ + GB and STZ + GR the cardiac MDA level was significantly lower than that in diabetic rats (*p* < 0.01).

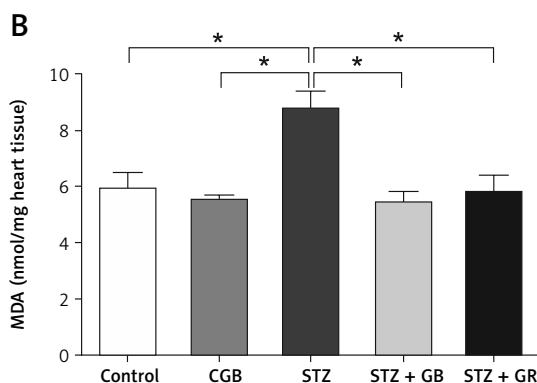
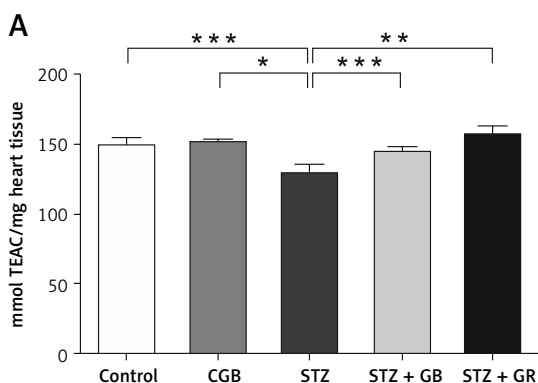


Figure 4. Antioxidant capacities of cardiac tissue homogenate of control, CGB, STZ, STZ + GB and STZ + GR groups at 8 weeks (A). The TEAC levels in diabetic in STZ rats were significantly decreased when compared with control and CGB groups (*p* < 0.05 and *p* < 0.001 respectively). Also, treatment diabetic rats in STZ + GB and STZ + GR groups had slightly higher TEAC levels (*p* < 0.05 and *p* < 0.001 respectively) compared to diabetic rats. Diabetic rats exhibited increase in cardiac MDA levels versus the control and CGB rats (*p* < 0.01) (B). However, STZ + GB and STZ + GR rats were significantly decreased in cardiac MDA compared with diabetic rats (*p* < 0.01). Values are mean ± SE

Determination of inflammatory cytokine

Cardiac inflammation is involved in diabetic cardiomyopathy. We analyzed the levels of the pro-inflammatory cytokines TNF- α and IL-1 β in the cardiac tissue. The diabetic rats developed myocardial inflammation as evidenced by significantly increased levels of cardiac TNF- α and IL-1 β compared to control rats ($p < 0.001$ and $p < 0.0001$ respectively). However, the myocardial TNF- α and IL-1 β levels were significantly decreased in diabetic rats treated with glabridin in STZ + GB rats ($p < 0.001$ and $p < 0.05$).

Immunofluorescence study

Increased expression of VEGF (bright green staining) in LAD was observed mainly in the smooth muscle layer of the arterial walls and endothelial cells in DM rats (Figure 5 C). The immunohistochemical section of LAD in control (Figure 5 A) and CGM (Figure 5 B) displayed a small amount of VEGF-specific antibody. Quantification of VEGF expression (Figure 5 B) showed a significant increase in diabetic rats over control rats ($p < 0.0001$). After the supplementation of glabridin (Figure 5 Ad) and glyburide (Figure 5 Ae), VEGF expression was significantly decreased compared with DM rats ($p < 0.0001$). According to TGF- β 1 expression (bright red staining), the internal elas-

tic lamina and smooth muscle layer of LAD walls were presented in STZ group (Figure 5 Ah). The immunohistochemical section of LAD in control (Figure 5 Af) and CGB (Figure 5 Ag) displayed a small amount of TGF- β 1 specific antibody. In diabetic rats the concentration of TGF- β 1 increased in the walls of LAD (Figure 5 Ah and IA (6C). Quantification of TGF- β 1 excretion (Figure 5 C) showed a significant increase in diabetic rat as compared to the control ($p < 0.001$). After the supplementation of glabridin (Figures 5 Ai) and glyburide (Figures 5 Aj), the intensity was significantly decreased in GM and GR rats ($p < 0.001$) (Figure 5 C).

Vascular corrosion cast examination

Comparing the vascular cast of the heart in control (Figure 7 A) and CGB (Figure 7 B) groups, heart microvasculature of the STZ group demonstrated the pathology and destruction of microvascular architecture in diabetic rats. The dense capillary network was gradually decreased in number. Arterial notch, stenosis, and shrinkage of the LAD were revealed (Figure 7 C). The LAD became irregular in caliber. Moreover, the neovascularization of nourishing blood vessels occurred and appeared extensively (Figures 8 A, B). Interestingly, the STZ group significantly revealed shrinkage and smaller sizes of proximal and distal

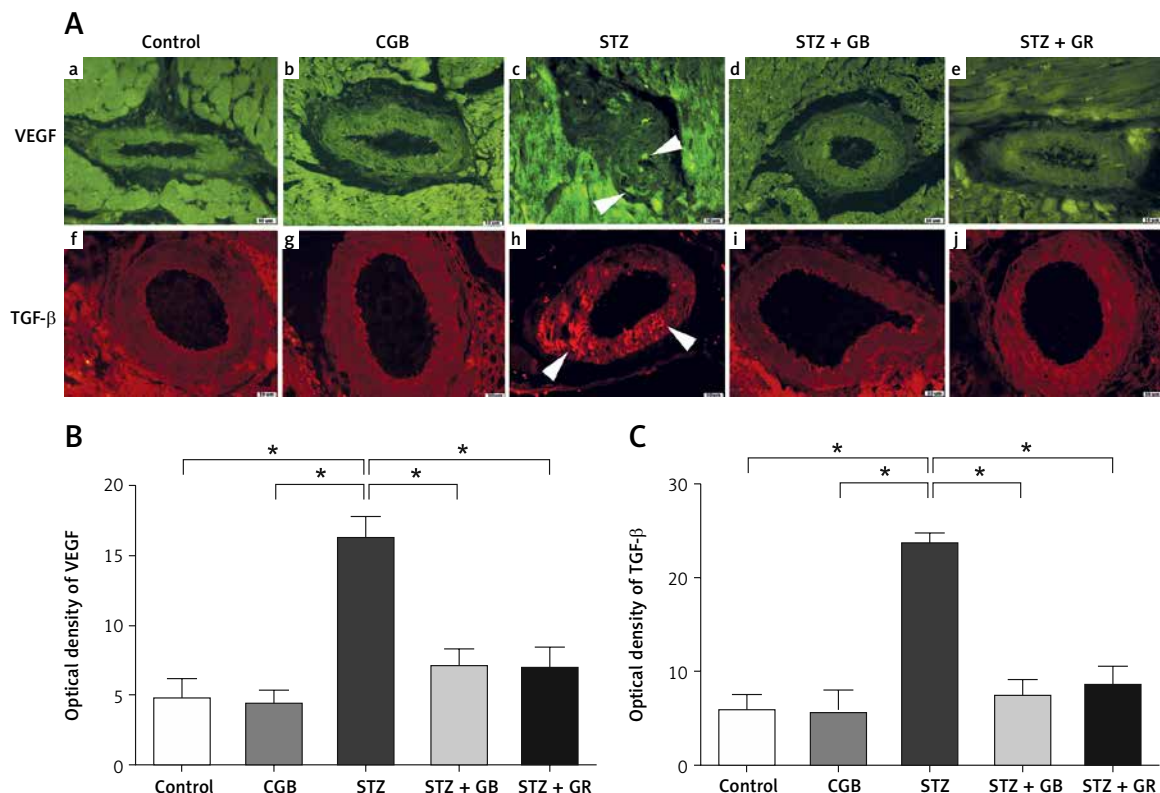


Figure 5. A – Photomicrographs of immunohistochemical sections of LAD with VEGF specific and TGF- β antibodies in rat kidneys. White arrowheads indicate an example of VEGF-immunoreactive smooth muscles in tunica media in STZ group. Relative VEGF (B) and TGF- β (C) optical density were analyzed. Values are mean \pm SE, *** $p < 0.001$ compared with control and STZ groups

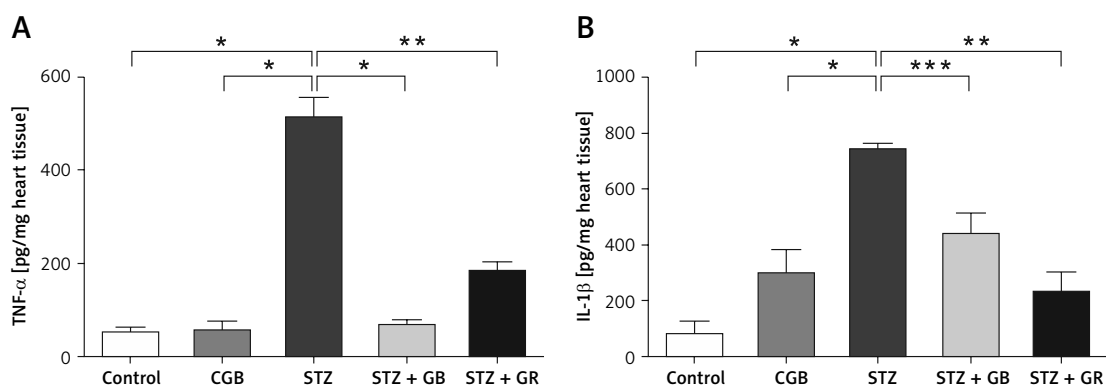


Figure 6. Levels of pro-inflammatory cytokines TNF- α (A) and IL-1 β (B) in the cardiac tissue of control, CGB, STZ, STZ + GB and STZ + GR groups at 8 weeks. The STZ group had significantly increased levels of cardiac TNF- α and IL-1 β versus control rats ($p < 0.001$ and $p < 0.0001$ respectively). However, the myocardial TNF- α and IL-1 β levels were significantly decreased in STZ + GB rats ($p < 0.001$ and $p < 0.05$). Values are mean \pm SE

parts of the LAD compared with the control and CGB groups. Fascinatingly, heart microvasculature in glabridin (Figure 7 D) and glyburide (Figure 7 E) treated groups was developed into remodeling and healthy characteristics, respectively. Concerning the sizes of the LAD, the average diameters of all groups were measured and compared (Figure 7 F). The STZ group demonstrated a decreased LAD diameter. Quantification of the diameter showed a significant decrease in diabetic rat as compared to control and CGB groups ($p < 0.001$). After the supplementation of glabridin and glyburide, the diameter was significantly increased compared with the STZ group ($p < 0.001$ and $p < 0.05$ respectively).

Western blot analysis

Western blot analysis revealed that VEGFA had a molecular weight of 27 kDa, TGF- β 1 had a molecular weight of 44 kDa, and the housekeeping protein, actin, had a molecular weight of 43 kDa in the control, CGB, STZ, STZ + GB and STZ + GR samples (Figure 9 A). The results demonstrated increased protein expression levels of VEGFA and TGF- β 1 in the STZ rats compared with the control, CGB, STZ, STZ + GB and STZ + GR rats. Furthermore, protein expression levels of VEGFA and TGF- β 1 decreased in the STZ + GB and STZ + GR groups following treatment with glabridin and glibenclamide compared with STZ rats. The protein expression levels of VEGFA and TGF- β 1 significantly increased in STZ rats compared with the control ($p < 0.0001$). Furthermore, VEGFA and TGF- β 1 protein expression levels significantly decreased in STZ + GB and STZ + GR rats compared with the STZ rats ($p < 0.01$ and $p < 0.001$, respectively) in Figure 9 B.

Discussion

The main risk factor for CAD is diabetes mellitus, which is associated with hyperglycemia [18].

Hyperglycemia, the hallmark of diabetes, promotes many variations in vascular tissue that potentially induce advanced atherosclerosis [19]. In diabetes, the extensive mechanisms important for the increased atherosclerosis is the nonenzymatic reaction of lipoproteins or between proteins and glucose in the walls of arteries [19]. We accomplish biochemical analyses, immunofluorescence, detection of inflammatory cytokines, and vascular corrosion cast after exposure to the STZ cytotoxic agent with the purpose of providing insight into the alleviated vascular inflammation of glabridin treatment in the heart over the course of 8 weeks. We observed that glabridin-treated STZ rats, compared with STZ rats, exhibited: (a) decreased blood glucose and blood cholesterol levels; (b) an increased antioxidant parameter; (c) decreased products of lipid peroxidation during oxidative stress; (d) remodeling of LAD; (e) amelioration of VEGF, TGF- β 1, collagen I, TNF- α and IL-1 β expression levels.

Blood cholesterol levels is important to overall health, but with exceeding levels cholesterol can be harmful by contributing to narrowed or blocked arteries. More than 97% of patients with diabetes are diagnosed with dyslipidemia [20]. Dyslipidemia is highly correlated with atherosclerosis, increased triglycerides and decreased HDL cholesterol. Insulin promotes the activity of the enzyme lipoprotein lipase, which mediates free fatty acid uptake into adipose tissue and suppresses the activity of the enzyme hormone-sensitive lipase, resulting in decreased release of free fatty acids into the circulation [21]. Normoglycemic individuals with dyslipidemia had no increase in MDA levels compared to normoglycemic individuals without dyslipidemia, indicating that the presence of hyperglycemia played a critical role in the increased MDA. Diabetes was significantly associated with lipid peroxidation markers, and a strong positive correlation was observed between MDA and glycated hemoglobin (HbA_{1c}) [22].

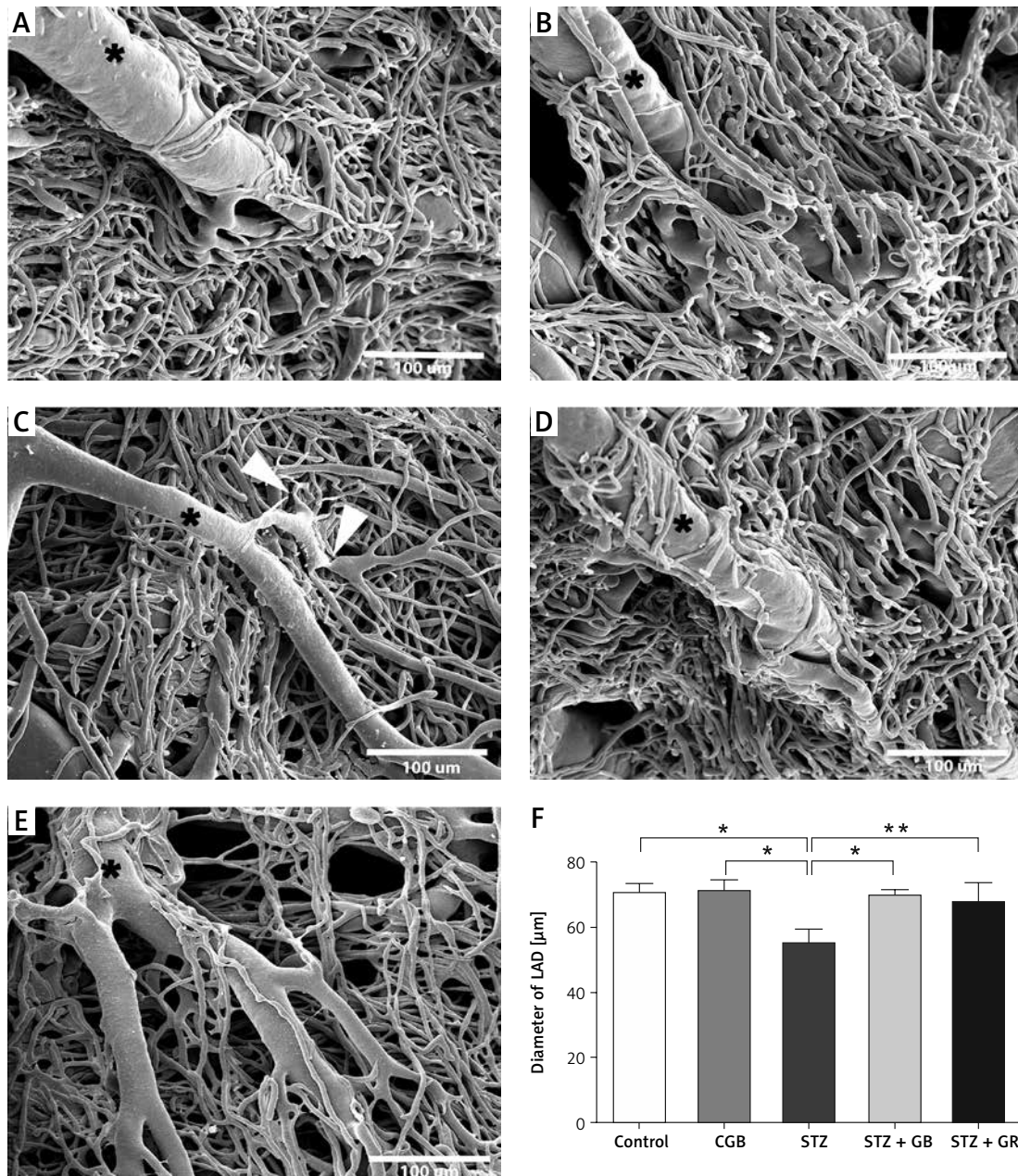


Figure 7. SEM micrographs of vascular cast of hearts in control (A), CGB (B), STZ (C), STZ + GB (D) and STZ + GR (E) rats. LAD supply blood flow to the anterior and anterolateral walls of the left ventricle (asterisk). In STZ rats, they revealed arterial notch, stenosis (white arrowhead), and shrinkage and had an irregular caliber. The average diameter showed a significant decrease in STZ versus control and CGB rats ($p < 0.001$). The diameters were significantly increased in STZ + GB and STZ + GR compared with STZ group ($p < 0.001$ and $p < 0.05$ respectively). Values are mean \pm SE

The present study used ABTS radical-scavenging activity to evaluate the antioxidant activity. Antioxidants present in the assayed tissue homogenates inhibit the oxidation of ABTS to ABTS+ to a degree that is proportional to their concentration. The capacity of the assayed sample antioxidants was compared with that of standard 6-hydroxy-2,5,7,8-tetramethylchroman-2-carboxylic acid (Trolox), a water-soluble tocopherol analogue, which is widely used as a traditional standard for TAC measurement assays. Glabridin treated dia-

betic rats had higher TEAC levels compared to diabetic rats, so that the treatment would provide anti-inflammatory activity with minimum toxicity. These results will be compiled into a database, and this method can therefore be a powerful pre-selection tool for compounds intended to be studied for their potential bioactivity and antioxidant activity related to their radical-scavenging capacity. These results agree with other works illustrating that glabridin possesses antioxidant properties studied in STZ induced diabetic animals [23].

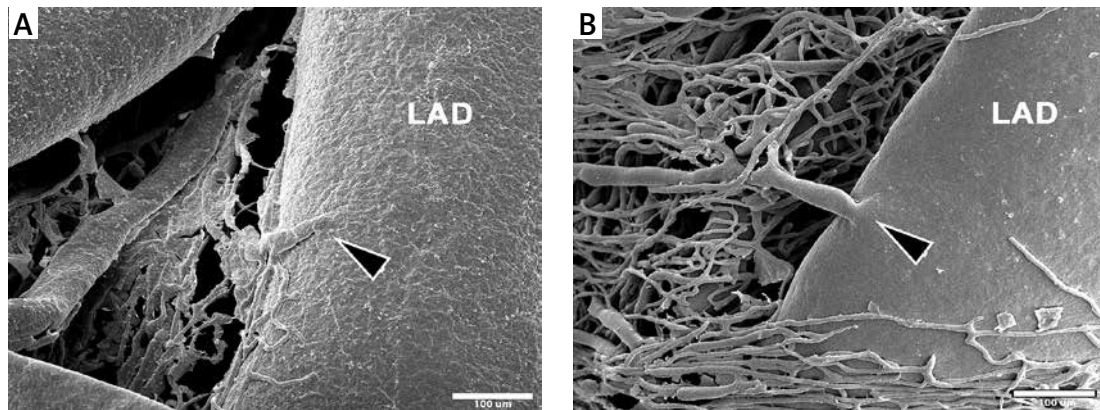


Figure 8. SEM micrographs of heart vascular corrosion cast in STZ rats (A, B). The sprouting of blood vessels from the LAD is presented (black arrowheads)

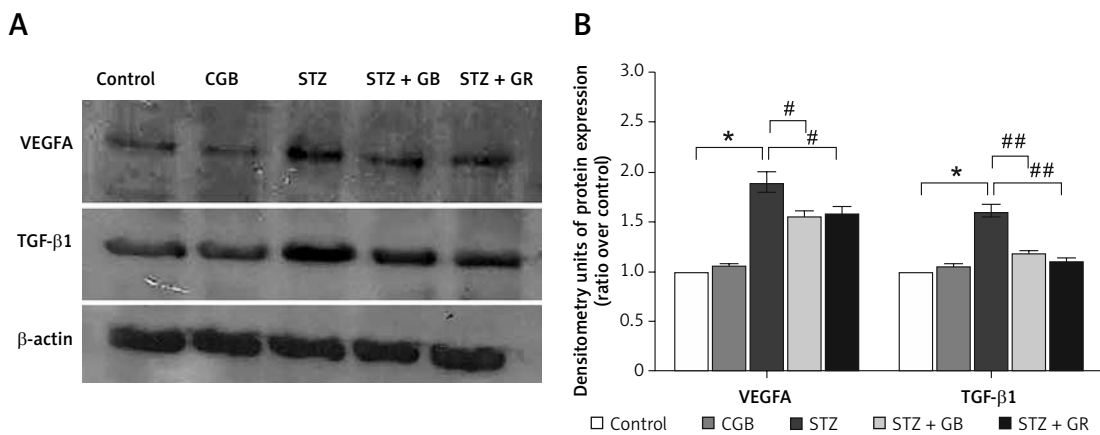


Figure 9. Western blot analysis (A) and densitometry of protein expression (B) demonstrated VEGFA, TGF-β1 and β-actin proteins from heart tissues at 8 weeks. Data are expressed as the mean ± standard error of the mean. * $P < 0.0001$, # $p < 0.01$ and ## $p < 0.001$

The possible linkage among inflammation, diabetes, and lipid peroxidation is demonstrated by a multiple regression analysis using separate models for independent variables. Lipid peroxidation markers and diabetic status were directly related to the expression of inflammatory cytokines, especially IL-1β and TNF-α [24].

In this experimental study, the histological observation as detected by Masson’s trichrome and H&E staining methods of the STZ group showed an increase in wall thickness of the LAD and the accumulation of collagen fibers. The pathogenic mechanisms for the microvascular complications in CAD may be associated with oxidative stress, which is regarded as the major factor that couples hyperglycemia with vascular complications. ROS is regulated by increased cytokine expression after vascular injury including TGF-β, basic fibroblast growth factor (bFGF), platelet-derived growth factor (PDGF), and Ang II [25]. Vascular injury is also increased by shear stress or mechanical disruption, as a result of which the artery is redeveloped by cells that move from bordering tissue [26].

The vascular cast and SEM demonstrated the characteristic LAD of STZ rats and revealed not only pathology and destruction but also neovascularization of the growing blood vessels from pre-existing vascular structures during treatment. Improvement of blood supply to ischemic myocardium can result from either true angiogenesis or from the recruitment of pre-existing coronary collateral vessels [27]. Oxygen plays a pivotal role in this regulation. Hemodynamic factors are critical for the survival of vascular networks and for structural adaptations of vessel walls. Specifically, glabridin is a potent anti-inflammatory, antioxidant agent and free radical scavenger [28]. The pathophysiologic effects of diabetes on the microcirculation of the heart may be reflected in the LAD vascular changes noted in this present study. Interestingly, healthy blood vessels recovered in in STZ + GB group. Regarding glabridin, it potentially suppressed lipid peroxidation after oral administration of ethanol extract of licorice root to healthy subjects for 6 months [29].

According to the immunofluorescence, western blot and ELISA analyses, VEGF is a major angiogen-

ic cytokine that plays a crucial role in blood vessel homeostasis and vascular diseases. VEGF normally relaxes the vascular tone and lowers the blood pressure by stimulating the release of nitric oxide, but diabetes promotes endothelial dysfunction and impairs the production of nitric oxide; thus uncoupling VEGF from nitric oxide provides beneficial effects. The VEGF effects are redirected toward endothelial cell proliferation, which has its deleterious consequences for diabetic vasculopathy [30]. TGF- β is an essential regulator of cell differentiation, phenotype, and function, which is implicated in the pathogenesis of many diseases. Myocardial infarction is associated to induce TGF- β 1, TGF- β 2, and TGF- β 3. TGF- β s regulate cardiomyocyte survival, promote monocyte chemotaxis, and modulate lymphocyte differentiation and activation. TGF- β may be critical in modulating macrophage phenotype toward an anti-inflammatory M2 phenotype. These effects may act as a switch from inflammation to repair [31] and were shown in experimental models of myocardial infarction, induction, and release of the pro-inflammatory cytokines such as TNF- α , IL-1 β and IL-6 [32]. Licorice extract and its bioactive components downregulate the expression levels of pro-inflammatory cytokines, including TNF- α , IL-1 β and IL-6 in induced liver damage model [33]. Glabridin has shown efficacy in decreasing various diabetic complications.

In conclusion, the present study showed the efficiency of glabridin treatment in beneficially repairing and regenerating LAD in diabetic animal hearts. It would be beneficial in examining the role of glabridin as a therapeutic aim in diabetes treatment research in CAD.

Acknowledgments

This research was supported by a grant from Prince of Songkla University Research Fund under grant no. SCI6202011S.

Conflict of interest

The authors declare no conflict of interest.

References

1. Chu Z, Yang Z, Dong Z, et al. Characteristics of coronary artery disease in symptomatic type 2 diabetic patients: evaluation with CT angiography. *Cardiovasc Diabetol* 2010; 9: 74.
2. Go AS, Mozaffarian D, Roger VL, et al. Heart disease and stroke statistics--2014 update: a report from the American Heart Association. *Circulation* 2014; 129: e28-292.
3. Aronson D, Edelman ER. Coronary artery disease and diabetes mellitus. *Cardiol Clin* 2014; 32: 439-55.
4. Chu Z, Yang Z, Dong Z, et al. Characteristics of coronary artery disease in symptomatic type 2 diabetic patients: evaluation with CT angiography. *Cardiovasc Diabetol* 2010; 9: 74.
5. Yusuf Muharam M, Ahmad R, Harmy M. The 'widow maker': electrocardiogram features that should not be missed. *Malaysian Fam Physician* 2013; 8: 45-7.
6. O'Keefe Jr JH, Kreamer TR, Jones PG, et al. Isolated left anterior descending coronary artery disease. *Circulation* 1999; 100 (Suppl 2): II-114-8.
7. Mahmarian JJ, Pratt CM, Boyce TM, Verani MS. The variable extent of jeopardized myocardium in patients with single-vessel coronary artery disease: quantification by thallium-201 single photon emission computed tomography. *J Am Coll Cardiol* 1991; 17: 355-62.
8. Cameron A, Davis KB, Green G, Schaff HV. Coronary bypass surgery with internal-thoracic-artery grafts: effects on survival over a 15-year period. *N Engl J Med* 1996; 334: 216-9.
9. Virdis A, Schiffrin EL. Vascular inflammation: a role in vascular disease in hypertension? *Curr Opin Nephrol Hypertens* 2003; 12: 181-7.
10. Uitto J, Perejda AJ, Grant GA, Rowold EA, Kilo C, Williamson JR. Glycosylation of human glomerular basement membrane collagen: increased content of hexose in ketoamine linkage and unaltered hydroxylysine-Oglycosides in patients with diabetes. *Connective Tissue Res* 1982; 10: 287-96.
11. Nishikawa T, Edelstein D, Du XL, et al. Normalizing mitochondrial superoxide production blocks three pathways of hyperglycaemic damage. *Nature* 2000; 404: 787-90.
12. Gupta SC, Patchva S, Aggarwal BB. Therapeutic roles of curcumin: lessons learned from clinical trials. *AAPS J* 2013; 15: 195-218.
13. Shang H, Cao S, Wang J, et al. Glabridin from Chinese herb licorice inhibits fatigue in mice. *Afr J Tradit Complement Altern Med* 2009; 7: 17-23.
14. Choi EM. The licorice root derived isoflavan glabridin increases the function of osteoblastic MC3T3-E1 cells. *Biochem Pharmacol* 2005; 70: 363-8.
15. Komolkriengkrai M, Nopparat J, Vongvatcharanon U, Anupunpisit V, Khimmaktong W. Effect of glabridin on collagen deposition in liver and amelioration of hepatocyte destruction in diabetes rats. *Exp Ther Med* 2019; 18: 1164-74.
16. Khan N, Akhtar MS, Khan BA, Braga V de A, Reich A. Antiobesity, hypolipidemic, antioxidant and hepatoprotective effects of *Achyranthes aspera* seed saponins in high cholesterol fed albino rats. *Arch Med Sci* 2015; 11: 1261-71.
17. Katalinic V, Modun D, Music I, Boban M. Gender differences in antioxidant capacity of rat tissues determined by 2,2'-azinobis (3-ethylbenzothiazoline 6-sulfonate; ABTS) and ferric reducing antioxidant power (FRAP) assays. *Comp Biochem Physiol C Toxicol Pharmacol* 2005; 140: 47-52. doi
18. Haberka M, Jankowski P, Kosior DA, et al. Treatment goal attainment for secondary prevention in coronary patients with or without diabetes mellitus – Polish multicenter study POLASPIRE. *Arch Med Sci* 2020. doi:10.5114/aoms.2020.92558.
19. Aronson D, Rayfield EJ. How hyperglycemia promotes atherosclerosis: molecular mechanisms. *Cardiovasc Diabetol* 2002; 1: 1. doi:10.1186/1475-2840-1-1.
20. Fagot-Campagna A, Rolka DB, Beckles GL, Gregg EW, Narayan KM. Prevalence of lipid abnormalities, awareness, and treatment in US adults with diabetes. *Diabetes* 2000; 49 (Suppl. 1): A78.
21. Shen G. Lipid disorders in diabetes mellitus and current management. *Curr Pharm Anal* 2007; 3: 17-24.
22. de Souza Bastos A, Graves DT, de Melo Loureiro AP, et al. Diabetes and increased lipid peroxidation are associat-

- ed with systemic inflammation even in well-controlled patients. *J Diabetes Complications* 2016; 30: 1593-9.
23. Wu F, Jin Z, Jin J. Hypoglycemic effects of glabridin, a polyphenolic flavonoid from licorice, in an animal model of diabetes mellitus. *Mol Med Rep* 2013; 7: 1278-82.
 24. Shi J, Fan J, Su Q, Yang Z. Cytokines and abnormal glucose and lipid metabolism. *Front Endocrinol* 2019; 10: 703.
 25. Papaharalambus CA, Griendling KK. Basic mechanisms of oxidative stress and reactive oxygen species in cardiovascular injury. *Trends Cardiovasc Med* 2007; 17: 48-54.
 26. Taylor WR. Hypertensive vascular disease and inflammation: mechanical and humoral mechanisms. *Curr Hypertens Rep* 1999; 1: 96-101.
 27. Tabibiazar R, Rockson SG. Angiogenesis and the ischemic heart. *Eur Heart J* 2001; 22: 903-18.
 28. Belinky PA, Aviram M, Fuhrman B, Rosenblat M, Vaya J. The antioxidative effects of the isoflavan glabridin on endogenous constituents of LDL during its oxidation. *Atherosclerosis* 1998; 137: 49-61.
 29. Carmeli E, Fogelman Y. Antioxidant effect of polyphenolic glabridin on LDL oxidation. *Toxicol Industrial Health* 2009; 25: 321-4.
 30. Nakagawa T. Uncoupling of the VEGF-endothelial nitric oxide axis in diabetic nephropathy: an explanation for the paradoxical effects of VEGF in renal disease. *Am J Physiol Physiol* 2007; 292: F1665-72.
 31. Hanna A, Frangogiannis NG. The role of the TGF- β superfamily in myocardial infarction. *Front Cardiovasc Med* 2019; 6: 140.
 32. Neri M, Fineschi V, Di Paolo M, et al. Cardiac oxidative stress and inflammatory cytokines response after myocardial infarction. *Curr Vasc Pharmacol* 2015; 13: 26-36.
 33. Yu JY, Ha JY, Kim KM, Jung YS, Jung JC, Oh S. Anti-inflammatory activities of licorice extract and its active compounds, glycyrrhizic acid, liquiritin and liquiritigenin, in BV2 cells and mice liver. *Molecules* 2015; 20: 13041-54.